Article

Study on the Expansion Potential of Artificial Oases in Xinjiang by Coupling Geomorphic Features and Hierarchical Clustering

Keyu Song [1,2], Weiming Cheng [1,2,3,4,5,*], Baixue Wang [1], Hua Xu [1,2], Ruibo Wang [1,6] and Yutong Zhang [1,2]

1   State Key Laboratory of Resources and Environmental Information System, Institute of Geographic Sciences and Natural Resources Research, Chinese Academy of Sciences, Beijing 100101, China; songkeyu21@mails.ucas.ac.cn (K.S.); wangbx.19b@igsnrr.ac.cn (B.W.); xuhua7121@igsnrr.ac.cn (H.X.); wangrb@lreis.ac.cn (R.W.); zhangyutong23@mails.ucas.ac.cn (Y.Z.)
2   University of Chinese Academy of Sciences, Beijing 100049, China
3   Jiangsu Center for Collaborative Innovation in Geographical Information Resource Development and Application, Nanjing 210023, China
4   Collaborative Innovation Center of South China Sea Studies, Nanjing 210093, China
5   Xinjiang Institute of Ecology and Geography, Chinese Academy of Sciences, Urumqi 830011, China
6   College of Geography and Remote Sensing Sciences, Xinjiang University, Urumqi 830046, China
*   Correspondence: chengwm@lreis.ac.cn

Abstract: The study of the expansion potential of artificial oases based on remote sensing data is of great significance for the rational allocation of water resources and urban planning in arid areas. Based on the spatio-temporal relationship between morphogenetic landform types and the development of artificial oases in Xinjiang, this study explored the development pattern of artificial oases in the past 30 years by using trend analysis and centroid migration analysis, constructing a series of landform–artificial oasis change indices, and investigating the suitability of different landforms for the development of artificial oases based on geomorphological location by adopting a hierarchical clustering method. The following conclusions are drawn: (1) From 1990 to 2020, the area of artificial oases in the whole territory continued to increase, with significant expansion to the south from 2005 to 2010. (2) Six categories of landform types for artificial oasis development were created based on the clustering results. Of these, 7.39% and 6.15% of the area's geomorphological types belonged to the first and second suitability classes, respectively. (3) The optimal scale for analyzing the suitability of landforms for the development of artificial oases over the past 30 years in the whole area was 8 km, which could explain more than 96% of the changes in the growth of artificial oases. The distribution of landforms of first- and second-class suitability within the 8 km buffer zone of an artificial oasis in the year 2020 was 10.55% and 9.90%, respectively, and landforms of first-class suitability were mainly concentrated in the near plain side of the urban agglomerations located on the northern and southern slopes of the Tianshan Mountains, and the urban agglomerations at the southern edge of Altai Mountains. This study quantified the potential of different geomorphological types for the development of artificial oases and provided a basis for site selection in future artificial oasis planning and urban construction.

Keywords: landscape type; land-use change; 1990–2020; change in gravity center; correlation analysis; development suitability

1. Introduction

An artificial oasis is an area suitable for human settlement and agricultural production that is considered the core of an arid area [1,2], and the expansion of artificial oases reflects the changes in population growth and urban production in the arid zone. Global climate change and the continuous development of urbanization have caused new changes and challenges to artificial oases [3], and oasis research has become a hot topic that has attracted extensive attention from scholars at home and abroad [4]. At present, studies on oasis

changes in arid zones have mainly focused on oasis vegetation [5–7], the dynamic monitoring of land-use changes [8–10], the driving factors of oasis land-cover changes [8,11–14], oasis desert mapping and evaluation [15,16], oasis carrying capacity, the development suitability scale [17–20], and oasis landscape pattern changes and ecological impacts [21], among other topics. In existing studies on artificial oases, Xinjiang, as a typical arid region in western China, has an important position in the study of Chinese oases.

Xinjiang is located in a vast inland arid zone, and with the in-depth implementation of the Belt and Road Initiative and the recent implementation of the overall program of the Xinjiang Pilot Free Trade Zone, population and urbanization problems have become more prominent, and the development of artificial oases in Xinjiang's arid zone has become an important strategic goal [22]. Scholars have conducted substantial research on artificial oases in Xinjiang. In the study of attribution of oasis migration changes, Zhang et al. examined land-change characteristics and the migration evolution process of the oases in Xinjiang from 1990 to 2020, and investigated the degree of influence of each factor on the spatial distribution of oasis migration by using geodetic probes [2]. A research group at the Xinjiang Institute of Ecology and Geography, Chinese Academy of Sciences studied and analyzed the relationship between oasis expansion and water resource use in the Manas River valley over the last 60 years [23]. Yao et al. analyzed remotely sensed ecological and land-cover data from 1990 to 2020 and concluded that human factors, such as the expansion of artificial oases into deserts, the replacement of desert ecosystems by agricultural ecosystems, and the increase in the distribution of impervious surfaces, dominated the distribution and changes in oases in Hota [24]. In the study of oasis development modes, Luo proposed oasis development modes such as the intensive land-use mode of the alluvial flood fan, the moderate agricultural development mode of the alluvial plain, and the ecological land-use mode of the river-end oasis [9]. Song et al. used the Automata–Markov model to simulate the future development of a typical artificial oasis and its landscape ecological pattern under different scenarios in the Northwest Alar Reclamation Area, and put forward recommendations for the development of the oasis under different scenarios [25]. Zhang et al. used a constructed oasis transition network to study the oasis transition processes and structural stability at the Tuha Basin between 1990 and 2020 [14].

However, most of the current studies on the expansion of artificial oases in Xinjiang have focused on the impact of factors such as population [26,27], economy [27], hydrological river network [20,28,29], and road traffic [4,30] on oasis development. There are fewer studies on geomorphological factors, and most of the existing studies face morphological and geomorphological constraints such as altitude [2,25,31], degree of slope [25,32], impact on the density of land use [33], and suitability assessment [34] level. Although the role of morphogenetically coupled geomorphological types in oasis development has been mentioned in relevant studies [9], research on the expansion dynamics of oasis development, including potential quantitative research on the geomorphologic coupling of land use and artificial oases, is still insufficient, while the degree of influence and the relationship between morphogenetic and geomorphological types on the development of artificial oases is not clear. Unlike other plain and hilly areas in eastern China with superior natural conditions, the unique and rich morphogenetic landforms in the arid zone of Xinjiang, which were created by the geological structure of mountainous basins and multiple main forces due to water flow, wind, and dryness, are a synthesis of hydrology, climate, elevation, undulation, soil, vegetation, and other natural factors, and contain multiple integrated information on natural geography. Studying the temporal and spatial relationships between morphogenetic landforms and the dynamic development of artificial oases in Xinjiang will help to understand the influence of the arid zone's subsurface background state on the development potential of artificial oases, which will enable the development of land of different morphogenetic landform types according to local conditions; this is of great significance for the future development and utilization of artificial oases in Xinjiang.

Therefore, this study used secondary land-use data of Xinjiang in 1990, 1995, 2000, 2005, 2010, 2015, and 2020, combined with morphogenetic landform data [35], to construct the coupling relationship of landforms, land use, and artificial oases. For the landform–artificial oasis change index, we clustered the geomorphological types that contribute to and affect the development speed of artificial oases, analyzed the distribution of suitable geomorphological types in the whole area, and conducted research on the expansion potential of Xinjiang's artificial oases under the influence of geomorphology, with the aim of providing a scientific guideline for the development of Xinjiang.

2. Data and Methodology

2.1. Study Area

Xinjiang is located in the hinterland of the Asian–European continent in the northwest of China, with a geographical location of 73°40′E~96°23′E, 34°22′N~49°10′N. It covers an area of 1,660,000 square kilometers, accounting for one-sixth of the country's total land area, and is a typical arid zone. Its climate is a typical temperate continental climate with low precipitation, high evaporation, and large temperature differences between day and night.

The Altai, Tianshan, and Kunlun Mountains are located in the north, middle, and south of Xinjiang, dividing the region into north and south, and the Junggar and Tarim basins are located in the north and south, respectively, showing the topographic characteristics of "three mountains and two basins" (Figure 1). These areas are divided into five first-class geomorphological landforms according to the theory of geomorphological zoning [36]. Seasonal flows and perennial rivers in the mountains create lake-formed landscapes and fluvial landscapes at the basin margins, the perennial arid environment develops extensive wind-formed and dry landforms in the basin, and the high-altitude areas in the mountainous regions develop into glaciers and ice-margined landforms covered with snow and ice all year round. Different genesis types combined with altitude and undulation characteristics form a rich and unique morphogenetic landform type in Xinjiang.
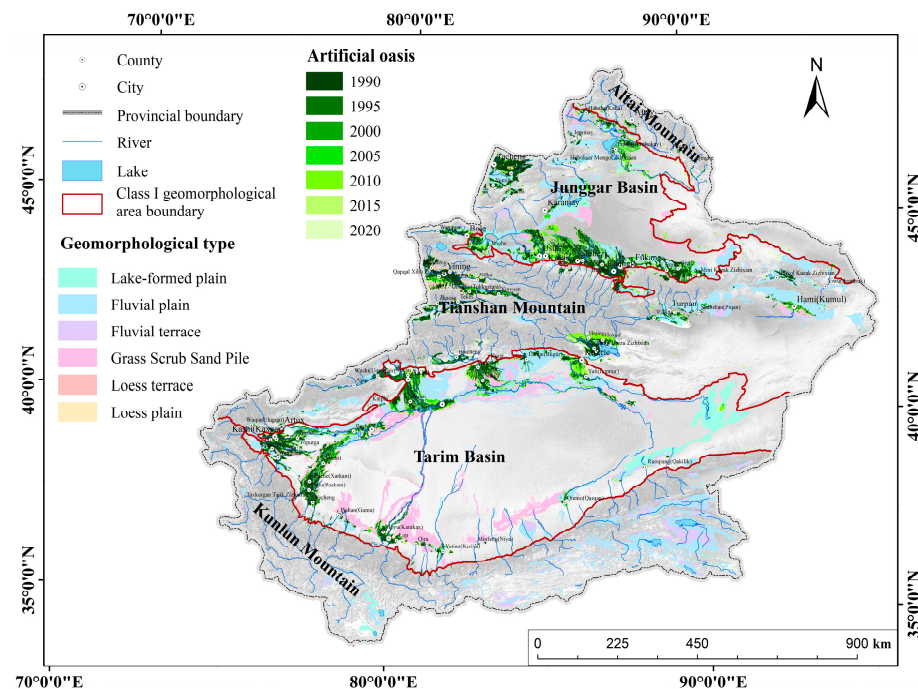

Figure 1. Overview of the study area.

Oases are usually formed in the plains of Xinjiang, where the terrain is gentle and water is abundant, and are divided into artificial oases and natural oases according to the degree of human interference, with less than 10 percent of their area supporting more than

90 percent of the population living in this arid zone. Most of the population and economic activities are concentrated in these artificial oases.

2.2. Datasets
2.2.1. Oasis Dataset

The oasis data for the study area were obtained as multi-period land-use/land-cover remote sensing data (CN-LUCC) from China's Resource and Environment Science Data Center of the Chinese Academy of Sciences and the Global Surface Cover Data Product Service website of the National Center for Basic Geographic Information (http://www.resdc.cn, accessed on 17 February 2022). A total of seven periods of land-use data (Figure 1) were selected, namely, 1990, 1995, 2000, 2005, 2010, 2015, 2020, and 2020. The interpretation of the 1990–2010 period mainly used Landsat TM/ETM series remote sensing data, and for the period 2015–2020, the analysis mainly used the latest Landsat-8 remote sensing image data, with a spatial resolution of 30 m. As one of the most accurate remote sensing monitoring datasets in China, CN-LUCC has been proven to have classification accuracies higher than 93% for the first level and higher than 90% for the second level through random sampling verification and Kappa coefficient accuracy assessments [37,38].

The land-use types were classified based on the classification system currently adopted by the Chinese Academy of Sciences, which consists of 6 categories of first-level land classes (cropland, forest land, grassland, watershed, construction land, and unused land) and 25 categories of second-level land classes. According to the hierarchy of oasis delineation in related studies [8,17], artificial oases and other types were established after merging the second level of the land-use data, in which artificial oases consisted of cropland (paddy field and dry land), forest land (other forest land), watershed (river canals, reservoirs, and ponds), and construction land (urban land, rural settlements, and other built-up land).

2.2.2. Geomorphological Data Products

Geomorphological data were obtained from the monograph "Geomorphological Patterns and Effects in Xinjiang" [35]. The main genesis types of landforms in Xinjiang include nine categories: fluvial, lake-formed, wind-formed, arid, glacial, ice-marginal, loess, volcanic lava, and karst [35] (Table 1). There are almost no volcanic lava and karst landforms due to the smaller area of artificial oases; thus, these landforms were simplified and ignored in subsequent calculations. Glacial landforms and ice-marginal landforms were developed in similar locations, whose environments are not conducive to the development of artificial oases, so they were combined into one category to simplify the analysis. Each landform contains different modes of action as their main force, such as the fluvial landform exhibits alluvial, flood, alluvial plus flood, erosion and denudation, and other modes of action as its main force. The main force's type plus mode of action together constitutes the genesis types of landforms in Xinjiang.

Table 1. Distribution of geomorphic landform types in Xinjiang.

Genesis Type	Fluvial	Wind-Formed	Arid	Ice-Marginal	Glacial	Loess	Lake-Formed	Karst	Volcanic Lava
Area/10^4 km^2	44.48	43.01	42.71	15.15	11.32	3.78	3.31	0.12	0.09
Percentage/%	27.12	26.27	26.03	9.24	6.90	2.30	2.02	0.07	0.05

The macro-morphological landform types include plains (cutting depth < 30 m), terraces (cutting depth > 30 m), hills (undulating height < 200 m), and mountains (undulating height ≥ 200 m) [39], and the morphogenetic landform data used in the study combine the abovementioned genesis types and macro-morphological types (Figure 2).
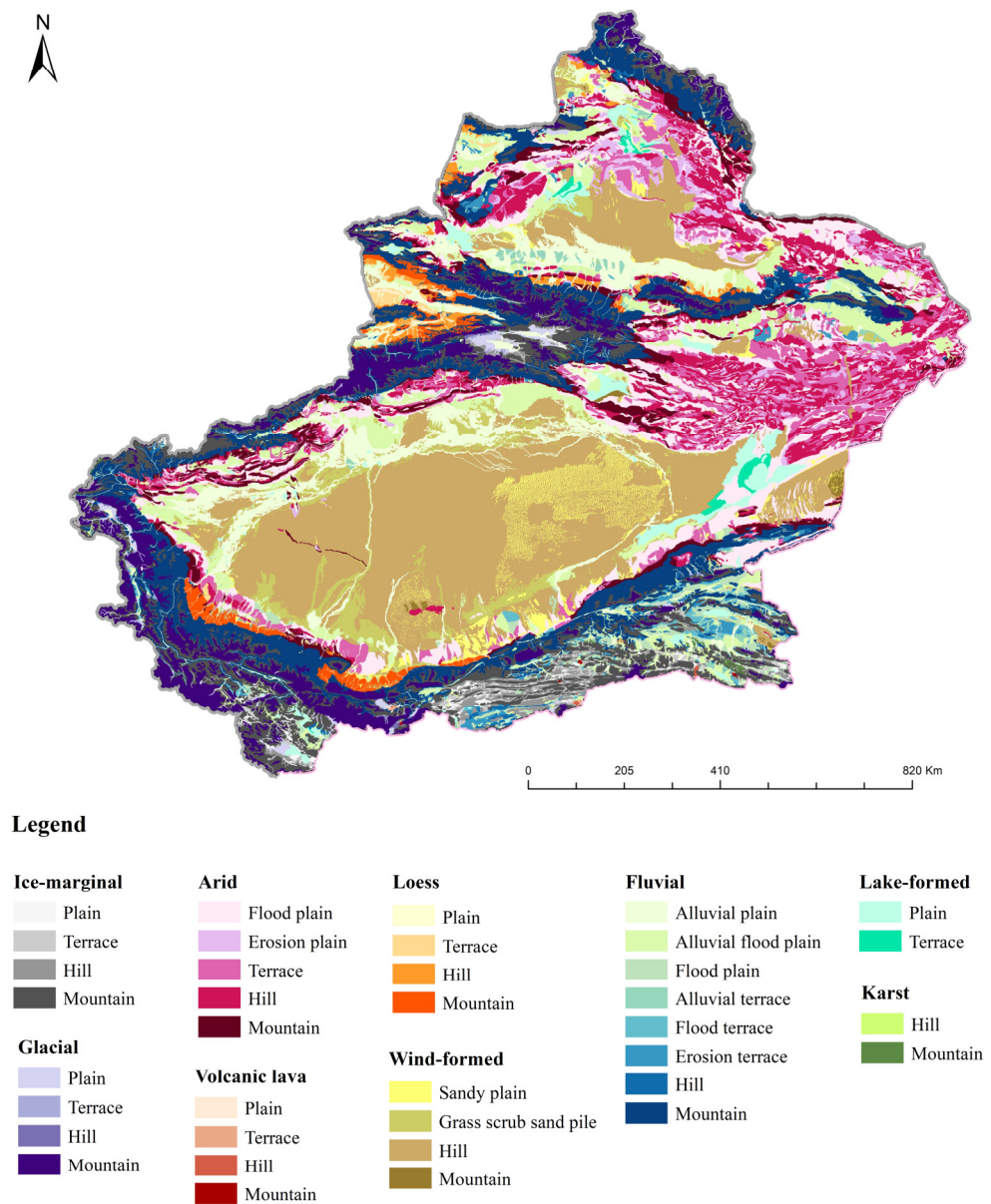
Figure 2. Geomorphological data showing types of macro-morphological landforms.

2.3. Methods

The experimental methodology used in this study consisted of three different stages (Figure 3): (1) data preparation and index establishment; (2) spatial and temporal variations and suitability analysis; and (3) development potential forecast.

2.3.1. Construction of Landform–Artificial Oasis Change Index

In this study, we used eight indices, namely, the dynamic amount of landform–artificial oasis change (ΔA_i), the rate of landform–artificial oasis change (ES_i), the index of landform–artificial oasis change trend (P_i), the index of bi-directional dynamic change in landform–artificial oasis expansion and contraction (TC_i), the contribution of landform–artificial oasis expansion ($Q_{e,i}$), the contribution of landform–artificial oasis contraction ($Q_{d,i}$), the total contribution of landform–artificial oasis change ($Q_{c,i}$), and the landform–artificial oasis exploitation degree index (D_{bi}), to measure the change in artificial oases under different morphogenetic landscapes.
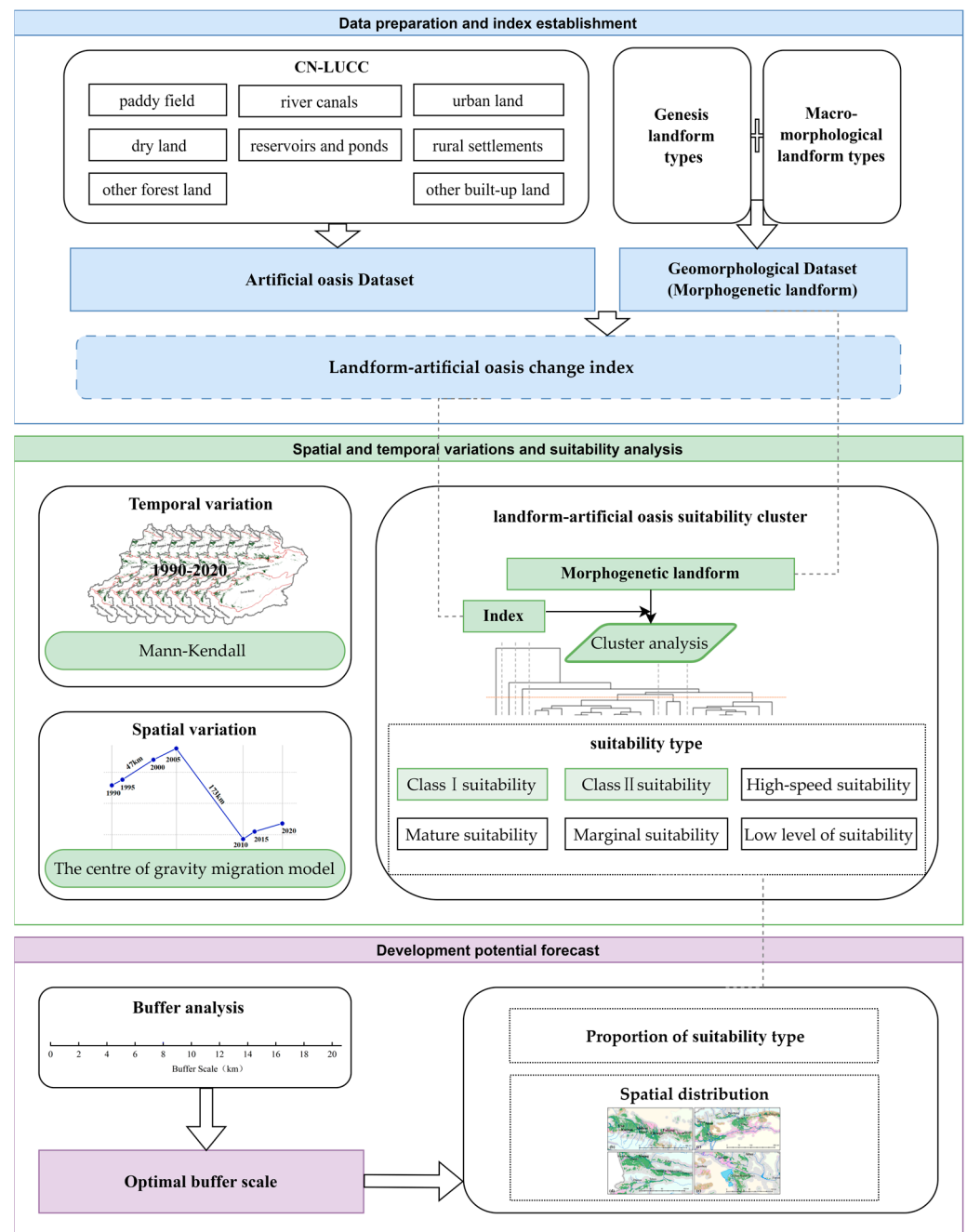
Figure 3. The methodological framework.

The change in an artificial oasis is a cumulative process, in which the change in area can reflect the change status of the artificial oasis during the study period. Drawing on the indicators of land-use change, we determined the dynamic degree of landform–artificial oasis change (ΔA_i), which is defined as the sum of change in terms of increase and decrease in an artificial oasis with a certain morphogenetic landform type over a period of time, and the formula is as follows:

$$\Delta A_i = \sum_{j=1}^{n} A_{bij} - \sum_{j=1}^{n} A_{aij} = \Delta A_{i-in} - \Delta A_{i-out} \tag{1}$$

where *i* describes a certain landform type; *i* denotes alluvial plains with fluvial action, eroded and denuded terraces with ice-marginal action, valley plains with arid action, or others; *j* is the *j*th landform patch under the *i*th landform type; a and b denote the years in the beginning and at the end of the study, respectively; and A_{bij} is the area of the artificial

oasis that belongs to the *j*th patch on the *i*th landform type in the year when the study ends. ΔA_{i-in} is the sum of the area converted from a non-artificial oasis to an artificial oasis in landform type *i* during the study period, ΔA_{i-out} is the sum of the area converted from an artificial oasis to other landforms in landform type *i* during the study period, which is known as shrinkage, and the difference between the two is the dynamic degree of landform–artificial oasis change.

To measure the rate of growth of an artificial oasis area in different landforms, analogous to urban studies, the geometric mean method of artificial oasis growth rate is used to estimate the rate of change in an artificial oasis of a particular landform type in the study area; the formula for calculating the rate of landform–artificial oasis change (ES_i) is as follows:

$$ES_i = \left(\sqrt[T]{\frac{\sum_{j=1}^n A_{bij}}{\sum_{j=1}^n A_{aij}}} - 1 \right) \times 100\% \tag{2}$$

where *T* is the length of the interval between the years *a* and *b*, and $ES_i > 0$ indicates an expansion of the oasis on landscape type *i*; the larger the value of ES_i, the greater the intensity of expansion. On the contrary, when $ES_i < 0$, it indicates a shrinkage of the oasis in this landform type; the larger the value of ES_i, the smaller the degree of shrinkage.

Based on the study of trends in land conversion status [10], the index of landform–artificial oasis change trend (P_i) is established as follows:

$$P_i = \frac{\Delta A_{i-in} - \Delta A_{i-out}}{\Delta A_{i-in} + \Delta A_{i-out}} \tag{3}$$

When $0 < P_i \leq 1$, the artificial oasis in landform type *i* develops in the direction of increasing scale; when $-1 \leq P_i < 1$, the artificial oasis develops in the direction of decreasing scale. When P_i is closer to 0, it indicates that the size of the artificial oasis is changing slowly, showing a state of equilibrium; when the value is closer to 1, it indicates that the main direction of development of this landscape is transitioning from a non-artificial to an artificial oasis, so the area of the artificial oasis is increasing steadily; when *Pi* is closer to -1, it indicates that the main change is transitioning from an artificial oasis or the landscape is not suitable for artificial use.

The index of the bi-directional dynamic change in landform–artificial oasis expansion and contraction (TC_i) is constructed to characterize the drastic degree of mutual transformation between artificial and non-artificial oases under a certain landform type, which can reflect which landform types belong to the hotspot landforms of changes in artificial oases. The index has the following expression:

$$TC_i = \left(\left(\left(\frac{\Delta A_{i-in} + \Delta A_{i-out}}{A_{ai}} \right) + 1 \right)^{1/T} - 1 \right) \times 100\% \tag{4}$$

where A_{ai} is the area of the artificial oasis in landform type *i* in the starting year of the study.

The contribution of landform–artificial oasis expansion ($Q_{e,i}$), the contribution of landform–artificial oasis contraction ($Q_{d,i}$), and the total contribution of landform–artificial oasis change ($Q_{c,i}$) were used to standardize the quantitative representation of the extent to which different landscapes contribute to changing artificial oases, with the following equations:

$$Q_{e,i} = \frac{\Delta A_{i-in}}{\Delta A_{in}} \times 100\% \tag{5}$$

$$Q_{d,i} = \frac{\Delta A_{i-out}}{\Delta A_{out}} \times 100\% \tag{6}$$

$$Q_{c,i} = \frac{\Delta A_{i-in} + \Delta A_{i-out}}{\Delta A_{in} + \Delta A_{out}} \times 100\% \tag{7}$$

where ΔA_{in} denotes the total area of change converted to artificial oases and ΔA_{out} represents the total area converted from artificial oases.

The landform–artificial oasis exploitation degree index (D_{bi}) is the percentage of the area of a certain landform that has been developed as an artificial oasis in relation to the total area of the landform, and its formula is as follows:

$$D_{bi} = \frac{A_{bi}}{G_i} \tag{8}$$

where A_{bi} is the area of artificial oases in landform type *i* in year *b* (2020), and G_i is the total area of landform type *i*.

2.3.2. Methods for Analyzing the Spatial and Temporal Distribution of Artificial Oases

The Mann–Kendall test [40,41] was used in the R-studio software (Version number: R-4.3.2) for trend analysis of temporal changes, which was used to determine whether the artificial oases across the whole territory exhibited a significant expansion or decay trend in the time series. The formulae are as follows:

$$S = \sum_{k=1}^{n-1} \sum_{j=k+1}^{n} sgn(A_j - A_k) \tag{9}$$

$$sgn(A_j - A_k) = \begin{cases} 1 & if\ A_j - A_k > 0 \\ 0 & if\ A_j - A_k = 0 \\ -1 & if\ A_j - A_k < 0 \end{cases} \tag{10}$$

The variance *VAR(S)* is calculated as follows:

$$VAR(S) = \frac{n(n-1)(2n+5)}{18} \tag{11}$$

The *Z*-statistic is defined as follows:

$$Z = \begin{cases} \frac{S-1}{\sqrt{VAR(S)}}, & S > 0 \\ 0, & S = 0 \\ \frac{S+1}{\sqrt{VAR(S)}}, & S < 0 \end{cases} \tag{12}$$

where A_j and A_k are the areas of the artificial oases in year *j* and year *k*, respectively; *n* is the number of years; *sgn* is the sign function; and the *Z*-statistic is significant at the given α level if $|Z| > u_{1-\frac{\alpha}{2}}$. The given significance level is $\alpha = 0.05$.

The center of gravity migration model [42] was used to reflect the process of spatial evolution of artificial oases; this model intuitively reflects the distribution pattern of artificial oases by calculating the center of gravity of the oases and deriving the transfer angle and migration distance.

2.3.3. Cluster Analysis

For the index of the spatio-temporal pattern of artificial oasis landforms, the hierarchical clustering method based on the average Euclidean distance between groups was used to classify different landforms into different types that are suitable for the development of artificial oases, and then different groups of landforms with different oasis development potential could be obtained. The main advantage of hierarchical clustering is that it does not require the number of clusters to be pre-defined [43]. Thus, scientific planning and construction can be carried out for different landform types and groups.

The basic principles of hierarchical clustering are as follows:

- Calculate the similarity matrix between individual landform–artificial oasis change indices corresponding to several landform types;
- Assume that each landform type is a cluster class;

- Cyclically merge the two clusters with the highest similarity and then update the similarity matrix;
- The loop terminates when the number of cluster classes is 1.

The order of cluster aggregation is visualized using a tree diagram, in which the merging algorithm is based on the similarity between clusters, i.e., the smaller the distance, the higher the similarity and the easier it is to classify them into one category. The similarity between clusters is calculated using the Euclidean distance method:

$$dist\left(P_i, P_j\right) = \sum_{k=1}^{n} (P_{ik} - P_{jk})^2 \tag{13}$$

where the distance between samples is $dist(P_i,P_j)$ and n is the number of landform types.

Clustering quality is assessed using the Silhouette coefficient [44]. For a dataset D of n objects, assume that D is divided into k clusters. For each object o in D, calculate the average distance $a(o)$ between the object and other objects in the cluster it belongs to. Similarly, calculate the minimum average distance $b(o)$ between the object and the clusters it does not belong to. For each object in the dataset, the Silhouette coefficient is calculated and then averaged as a measure of clustering quality. The Silhouette coefficient takes values in the range $[-1, 1]$, with values closer to 1 representing better-quality clusters and values closer to -1 representing worse-quality clusters.

$$S(i) = \begin{cases} 1 - \frac{a(i)}{b(i)}, & a(i) < b(i) \\ 0, & a(i) = b(i) \\ \frac{a(i)}{b(i)} - 1, & a(i) > b(i) \end{cases} \tag{14}$$

Here, $a(i)$ is the intra-cluster dissimilarity of sample i, which is the average distance from sample i to other samples in the same cluster; the smaller the value of $a(i)$, the greater the likelihood that sample i should be clustered into that cluster. $b(i)$ is the inter-cluster dissimilarity of sample i, with $b(i) = \min\{b_{i1}, b_{i2}, \ldots, b_{ik}\}$, in which b_{ij} is the average distance of all samples from sample i to another cluster C_j, i.e., the dissimilarity between sample i and cluster c_j; when $s(i)$ is close to 1, it indicates that it is reasonable for sample i to be clustered.

2.3.4. Analysis of the Development Potential of Artificial Oases in Different Landforms

The buffer function of ArcGIS was used to calculate the area of artificial oases in 2020 that were contained in buffer zones of different widths and distances in 1990, and to determine the most suitable study range for the expansion of artificial oases; on this basis, the buffer analysis were performed based on the artificial oases in 2020, and the area and spatial distribution of each suitable type within the width range were determined.

3. Results

3.1. Analysis of Spatial and Temporal Changes in Artificial Oases

The area of artificial oases in Xinjiang increased continuously for 30 years ($p < 0.05$), from 63,600 km^2 in 1990 to 64,000 km^2 in 1995 with a slow growth rate of 0.6%. From 2005 to 2010, there was an obvious expansion of artificial oases, whose growth rate reached the highest of 24.32% during the study period, which was closely related to the development of agricultural technology; a part of the second-class land suitable for land use was developed in large quantities, and the area of artificial oases increased to 93,600 km^2 in 2010. From 2010 to 2020, the growth rate slowed down, and the area of artificial oases reached 104,200 km^2 in 2020 (Figure 4a). The slowdown in the rate of growth was mainly due to the low agricultural efficiency and poor farming conditions of land on unsuitable artificial oasis landscapes in some areas, as well as the fact that some farmers had chosen to work as employees instead of farming. Although the trend of urban hardening of land was still on the rise, there were varying degrees of abandonment of arable land in some places. At the

same time, the government's ecological compensation policy had also slowed down the growth rate of artificial oases to some extent, and the ecological restoration of high-altitude and steep-slope landscapes continued. According to the Xinjiang Forestry Department, by the end of 2019, the cumulative area of plough-return, forest-return, and grassland-return areas in Xinjian had reached about 150 million ha [31].
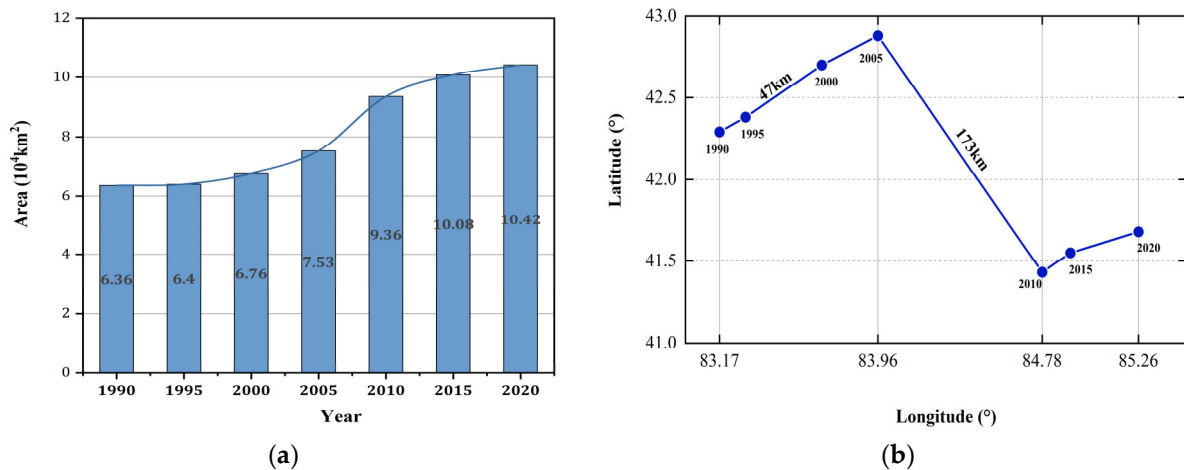

Figure 4. (**a**) Area change in artificial oases in Xinjiang from 1990 to 2020; (**b**) center of gravity migration of artificial oases in Xinjiang from 1990 to 2020.

We calculated the gravity center of artificial oases in period 7 (Figure 4b); the results showed that the gravity center of artificial oases continued to migrate in the northeast direction between 1990 and 2005, with a total migration of 90 km, of which the longest migration distance was 47 km between 1995 and 2000. The gravity center of artificial oases in this period was mainly affected by the expansion of the urban agglomeration located on the east northern slopes of Tianshan Mountains, with Urumqi as its representative. From 2005 to 2010, the gravity center of artificial oases shifted 173 km to 22.8 degrees southeast, which was the fastest growth period in the time series and was closely related to the development of oasis cities in the eastern part of the southern border of Xinjiang. Previously, arable land was mainly distributed in the alluvial flood plains of northern Xinjiang with favorable climatic conditions and suitable soil. However, around 2010, with the emergence and promotion of drip irrigation technology, the level of agricultural technology in China improved significantly [31]. This allowed some of the unused land in flood plains, grasslands, and other landscapes with relatively poor moisture conditions in southern Xinjiang to be reclaimed as farmland or orchards, resulting in a significant increase in area and a shift of focus to the south.

From 2010 to 2020, the center of gravity of artificial oases continued to shift towards the northeast, with a shift of 17 km towards 43.8 degrees northeast from 2010 to 2015, and 31 km towards 62 degrees northeast from 2015 to 2020; the development of these oases was relatively stable during this period, and it was still the urban agglomeration on the northern slopes of the Tianshan Mountains that gained momentum across the whole of Xinjiang, showing the highest contribution to the distribution of the gravity center.

3.2. Analysis of Landform–Artificial Oasis Suitability Cluster

The subcategories of genesis geomorphology with prominent features in the index (the mode of action of the main force) were proposed separately; the hierarchical clustering method based on calculating the average Euclidean distance between the groups was used to cluster the landform types with artificial oases throughout the whole territory according to the eight landform–artificial oasis indices; vertical standardization was used for the convenience of the visual analysis to obtain the clustering results shown in Figure 5 below.
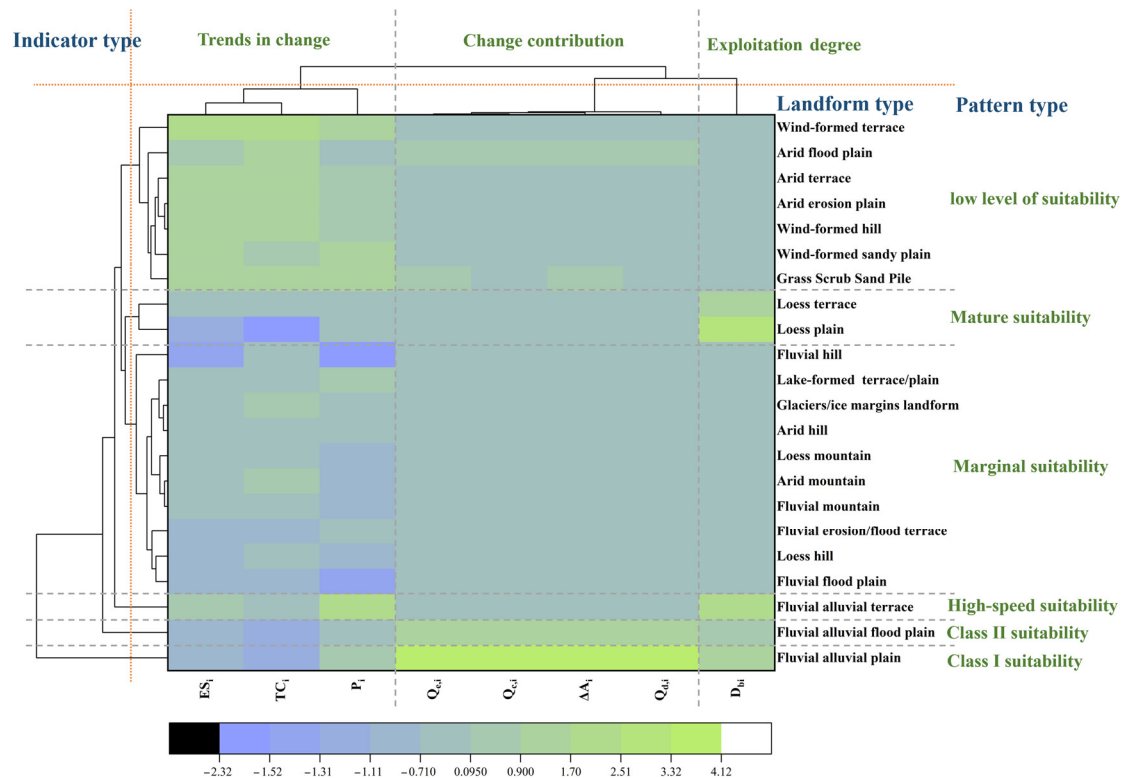
Figure 5. Landform–artificial oasis development suitability clustering heat map. The meanings of the indicators are as follows: the rate of landform–artificial oasis change (ES_i), the index of bi-directional dynamic change in landform–artificial oasis expansion and contraction (TC_i), the index of landform–artificial oasis change trend (P_i), the contribution of landform–artificial oasis expansion ($Q_{e,i}$), the contribution of landform–artificial oasis contraction ($Q_{d,i}$), the total contribution of landform–artificial oasis change ($Q_{c,i}$), the dynamic degree of change (ΔA_i), and the landform–artificial oasis exploitation degree index (D_{bi}).

The indicators were classified into three categories according to the similarity interpretation (Silhouette coefficient), namely, the category of indicators of trends of change, including the rate of landform–artificial oasis change (ES_i), the index of bi-directional dynamic change in landform–artificial oasis expansion and contraction (TC_i), and the index of landform–artificial oasis change trend (P_i); the category of indicators of change contribution change, including the contribution of landform–artificial oasis expansion ($Q_{e,i}$), the contribution of landform–artificial oasis contraction ($Q_{d,i}$), the total contribution of landform–artificial oasis change ($Q_{c,i}$), and the dynamic degree of change (ΔA_i); and the indicator in the exploitation degree category is the landform–artificial oasis exploitation degree index (D_{bi}).

According to the clustering results, the landform types were divided into six categories (Table 2), in which fluvial alluvial plains and fluvial alluvial flood plains were the main landform types contributing to the increase in artificial oases in the whole area, showing the first and second highest contribution to the change, respectively, along with a relatively high degree of development; these fluvial alluvial plains and fluvial alluvial flood plains were categorized as class I suitability and class II suitability of landform types suitable for the development of artificial oases, respectively. The overall area of fluvial alluvial terraces was not large and the degree of development was previously low, but the high rate of increase and the positive increasing trend in the last 30 years, coupled with a high degree of exploitation by the year 2020, made these terraces a landform type with high-speed suitability for the development of artificial oases. Loess plains and loess plateaus showed a slow growth rate and small changes, or even a negative growth trend, but they had a high degree of development and were landforms with a more mature development pattern.

Because land suitable for development into an artificial oasis had basically been fully developed, these plains and plateaus were categorized as a landform type with mature suitability. The overall change trend of artificial oases in the landform type of wind-formed terraces, arid flood plains, arid terraces, arid erosion plains, wind-formed hills, wind-formed sandy plains, and wind-formed grass scrub sand piles was large, but the proportion of artificial oases in this landform type was small and the degree of development was low, which meant that it had a low level of suitability and could be developed with the technical support of irrigation and other technologies. For the landform types with fluvial hills, lake-formed plains, glacial/ice-margins landforms, arid hills, loess hills, arid mountains, fluvial hills, fluvial erosion/flood terraces, loess hills, and fluvial flood plains, the area of artificial oases was small due to drought, altitude, and gravelly soils, among other reasons; these landform types were less utilized and were categorized as being of marginal suitability for the development of artificial oases. Landform types that had a low level of suitability or marginal suitability for the development of artificial oases accounted for more than 80 percent of the territory, which meant that most of the land in the territory was unsuitable for the development of artificial oases in terms of morphogenetic landform types.

Table 2. Patterns of landform types with suitability for the development of artificial oases.

Pattern Type	Code	Patterns of Temporal and Spatial Variation	Number of Landform Types	Area (km^2)	Percentage
Class I suitability	1	Maximum contribution to change, greater degree of exploitation	1	119,452.22	7.39%
Class II suitability	2	Second highest contribution to change, medium level of exploitation	1	99,459.08	6.15%
High-speed suitability	3	Rapid trend, low contribution to change, and high degree of exploitation	1	3819.29	0.24%
Low level of suitability	4	Rapid trend, low contribution to change, and little exploitation	7	677,558.12	41.89%
Mature suitability	5	Slow or even negative trend, low contribution, and high degree of exploitation	2	5659.78	0.35%
Marginal suitability	6	Slow or even negative trend, low contribution, and little exploitation	10	711,504.77	43.99%

3.3. Forecasting the Development Potential of Artificial Oases across the Territory Based on Geomorphological Conditions

The expansion of artificial oases is dominated by the outward expansion (marginal expansion) and infill (infill expansion) of the original artificial oases. Enclave expansion accounts for a relatively small proportion of expansion scenarios in most types of land, and at the same time, enclave expansion is more difficult to predict due to the uncertainty of the location in which it occurs; therefore, changes in land use in the vicinity of the original artificial oases were mainly considered in the present study.

A buffer zone with a width of 0.5–20 km was created at certain intervals for the artificial oases in 1990, and the area of artificial oases in 2020 within the buffer zones of different widths was calculated (Figure 6). The results showed that 72% of the area of artificial oases in 2020 was covered by artificial oases in 1990 and their surroundings within 0.5 km. The area of artificial oases in 2020 within a buffer zone increased as the buffer zone range increased, and the growth trend slowed down and stabilized while a large amount of the surrounding undeveloped open space was encompassed by the buffer zone. Thus, a buffer distance of 8 km was chosen for a comprehensive analysis. In this analysis, 96.02 percent of the area of artificial oases in 2020 fell within 8 km of the area of artificial oases in 1990 and their surroundings, and the 8 km buffer zone explained most of the change in area during the 30-year development of artificial oases.
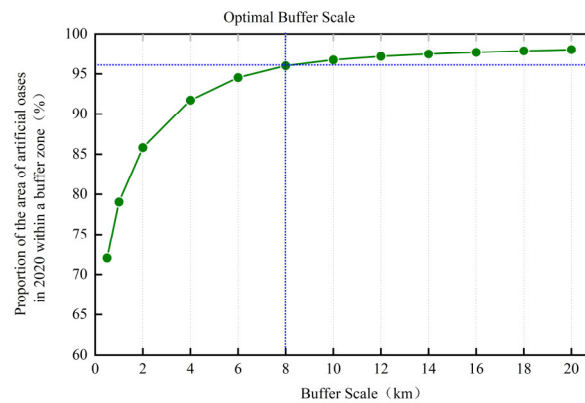
Figure 6. Relationship between the proportion of artificial oases in 2020 and the buffer scale.

Based on the area of artificial oases in 2020, an 8 km buffer zone was created, and the proportion and distribution of various types of geomorphologically suitable landform types within the buffer zone were calculated. In terms of area (Figure 7), landform types of high-speed suitability and mature suitability accounted for the smallest amount of area, at 0.3% and 0.7%, respectively, which was related to the fact that there are fewer places of these two landform types. The landform types of class I suitability and class II suitability accounted for 10.5% and 9.9%, respectively, and these were the most probable geomorphological landform types that could continue to be developed into artificial oases. Although the proportion of the distribution area of the landform types with class I suitability and class II suitability was larger near the original oases compared to the distribution in the whole territory, the suitability for development of these landform type was generally low because over half of the land was on the edge of an artificial oasis.
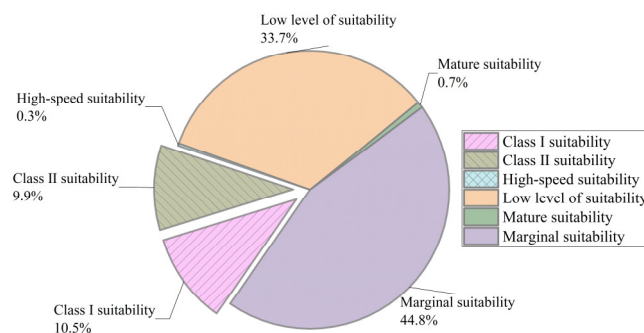

Figure 7. The proportion of landform types with suitability for the development of artificial oases within the 8 km buffer zone in 2020.

In terms of spatial location (Figure 8), there were lands on certain landform types that were suitable for development into artificial oases to some extent, including around the cities on the north and south sides of the Tianshan Mountains, especially north of Hutubi and Jimusar (Figure 8b), and there was a larger area of alluvial plains on the south of Shaya, which is located on the southern slopes of the Tianshan Mountains, that could be developed (Figure 8c). In the Tuha Basin, except for Torkun, which held a small amount of land with landforms of first-class suitability, there was very little land with landforms of class I suitability in other areas, and the majority of land suitable for development was dominated by landforms of second-class suitability. In the middle of the Tianshan Mountains, urban development was more complete, with less land belonging to the landforms of class I and class II suitability for development (Figure 8d). In the north of the border, the land available for development around Habaha and Buurzin was located in a large area of first-class suitability, and there was more than sufficient space for development (Figure 8e).
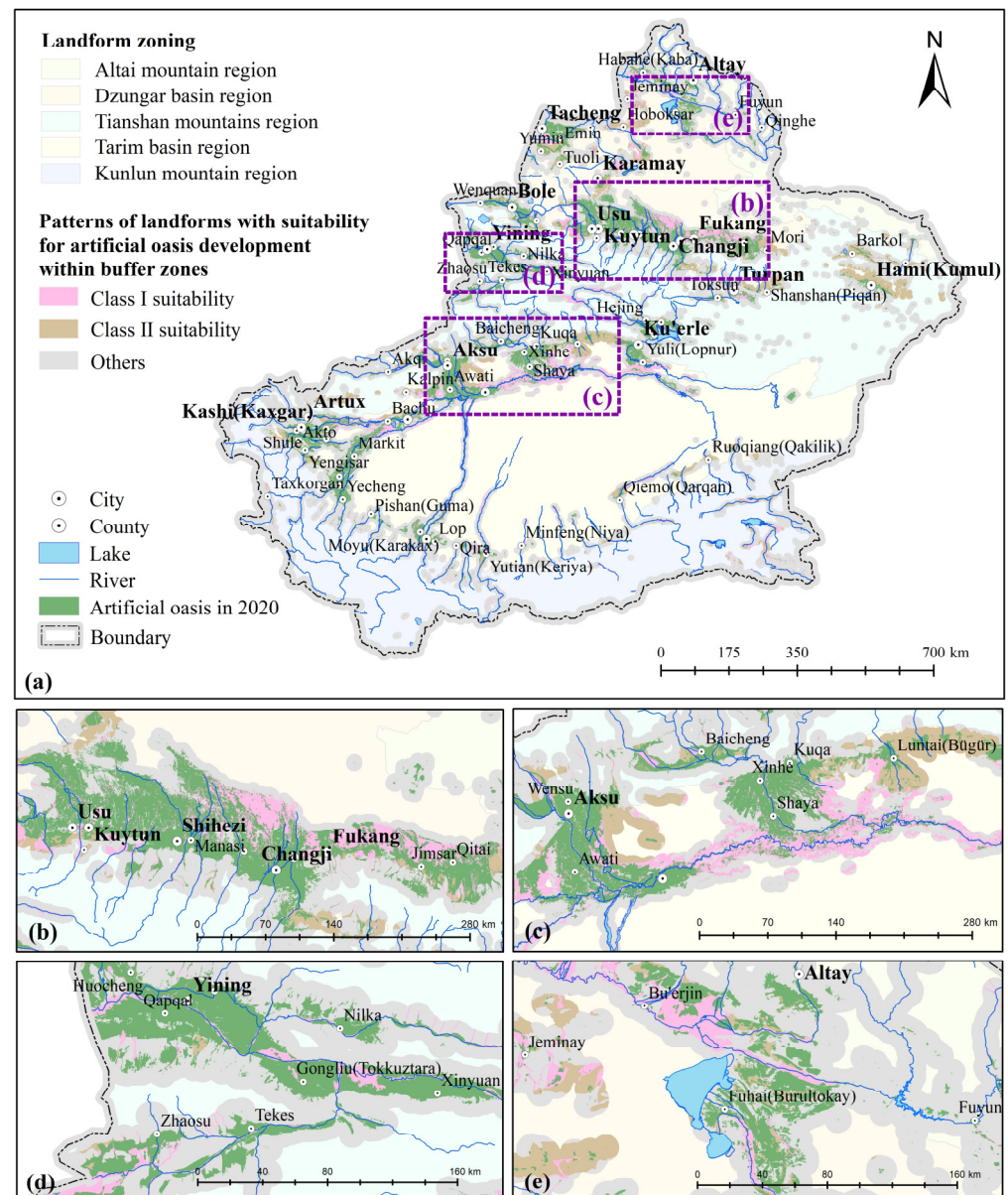
Figure 8. Distribution of landform patterns of primary and secondary suitability for development of artificial oases within the 8 km buffer zone of an artificial oasis in 2020 in Xinjiang (**a**–**e**). Figure (**b**–**e**) show partial enlargement of Figure (**a**), and the purple dotted boxes in Figure (**a**) show the overall positions of these landforms in Xinjiang. Figure (**b**) shows a part of the north slope of the Tianshan Mountains; Figure (**c**) shows a part of the south slope of the Tianshan Mountains; Figure (**c**) shows the Ili River Valley region; and Figure (**d**) shows the south of the Altai Mountains.

4. Discussion

4.1. Impact of Morphogenetic Landforms on Artificial Oasis Change

Since the 1990s, land use in Xinjiang has changed considerably, and scholars have examined change statistics from the perspectives of oases [45,46], arable land [13,27,29], and construction land [12,47] across the whole territory. Existing studies have found that the total area of artificial oases has substantially increased due to the development of agricultural technology before and after 2010, and the trend of southward movement is obvious in general [14,27]. However, most of the analyses on oasis changes in previous work only examined the time trend of oasis changes and the changes in the transfer matrix of land-use types, and there is a lack of separate analyses on the relationship between changes in artificial oases and geomorphological types. In terms of attribution

of oasis changes, previous studies have focused on multifactorial analyses of hydrology, climate, soil, economy, population, topographic relief, and elevation [48–50]. Topographic elevation and relief, as morpho-geomorphological elements, remain basically unchanged in a short period of time, which means they should be taken into account in the model as constraints, and it is difficult to use them as explanatory factors in attribution analyses of oasis dynamic changes.

However, for Xinjiang, the morphological factors of the terrain explain the expansion of artificial oases more than demographic and economic factors, as confirmed by previous studies [27], mainly because the special morphology of its mountainous areas and basins restricts the expansion of specific land-use types. Unlike plains where a flat river can expand uniformly in all directions, some of the artificial oases in Xinjiang will stop or slow down their expansion when they are blocked by mountains such as the Tianshan Mountains, Altay Mountains, and Kunlun Mountains, and the mountainous terrain also prevents the merging of these artificial oases on both sides, which reflects the influence of morphological landform types on the development of oases. In addition, water resources are one of the most important factors limiting the development of oases [14,51]. As the lifeline of irrigated agriculture, water determines the distribution of farmland [52], and without the support of water resources, arable land will be abandoned and degraded. For arid zones, the pattern of the landform greatly affects the distribution of water resources. For example, the edges of alluvial flood fans in these plains are often where groundwater is exposed, and these locations are also often where oases begin to appear [53,54], which fully reflects the influence of geomorphological structure on the distribution and development of artificial oases. The geomorphological genesis type indicates the role and mode of action of the main forces that caused the existing landform; for example, the fluvial landform type represents a landform type whose geomorphology is formed under the influence of flowing water, and the arid landform type is mainly molded by the erosion and stripping of the arid environment, which implies the current status and possible direction of utilization of water resources, and has a very strong indicative role in the potential development of artificial oases.

Unlike factors such as elevation and undulation, the genesis of morphological landforms has been included in few studies as a factor of artificial oasis development as it is a category variable rather than a numerical variable. However, the genesis of morphological landforms contains a lot of information; for example, the genesis of fluvial alluvial plains contains information such as relatively abundant water resources in terms of hydrology and loamy soil with fine soil grains, which have covariate relationships with other natural factors. This is different from the combination analysis of individual elements. By analyzing the morpho-geomorphological genesis of landforms as a whole, we can avoid the local bias of multi-factorial numerical computation and have a more holistic understanding, which is suitable for the analysis of the "object" rather than the calculation of individual "raster". This fully reflects the necessity of studying the genesis of landforms.

4.2. Explanation of Clustering Suitability Patterns

Many studies have analyzed the stability of oases from the perspective of ecological carrying potential using multi-indicator layers [55,56], and in terms of suitability research, some scholars have focused on the ratio of suitability between an artificial oasis and a natural oasis and proposed a balanced model of oasis development [18,22,34]; multi-indicator methods, such as hierarchical analysis methods, have been widely applied to the evaluation of suitability of a single land-use type [57,58]. However, this part of the study requires multi-source data, and the relationship between various indicators is complex, which makes it difficult to clarify the inclusion of interactive relationships. In these studies, clustering heat maps are often used as clusters of spatial objects [59,60] to achieve type classification based on indicators.

Based on the above shortcomings, this study innovatively introduced the index parameters of artificial oasis and morphogenetic landform types; by clustering the landform

types with artificial oasis in the whole territory according to the landform–artificial oasis change index, they can be divided into six categories of landform–artificial oasis types, and the most suitable landforms of the first and second classes for the development of artificial oases are fluvial alluvial plains and fluvial alluvial flood plains, which is in high agreement with the results of previous evaluation using multiple indicators [35]. In addition, fluvial alluvial terraces were classified as suitable geomorphological types for high-speed development, and loess plains and loess terraces are as landform types with mature suitability, which have obvious characteristics but are small in size and, thus, were not used in the main analysis on the suitability of geomorphological landforms for the development of artificial oases in the whole territory. The landform types with the largest percentage of area are unsuitable for the development of artificial oases (low level of suitability and marginal suitability); thus, the majority of land in the whole territory is restricted in terms of development of artificial oases.

Regarding the expansion mode of artificial oases, related studies have found that the artificial oasis development approach in Xinjiang represented by cultivated land shows obvious path dependence, and new artificial oases are mainly distributed in the periphery of the original oases [27]. However, there is a lack of study on the expansion range of specific artificial oases in the original developed land. Thus, this study investigated the expansion range during the development of artificial oases from 1990 to 2020 and found that an 8 km buffer zone around an original artificial oasis could explain more than 96% of the growth change in the next 30 years. Based on this result, the suitability of landform types within 8 km of an artificial oasis in 2020 was calculated. Compared to the scenarios of predictions based on suitability throughout the whole territory and future scenario modeling based on land-use types [61], this study avoids discrete locations far away from existing artificial oases and settlements, and the approach based on a priori statistics makes this study more relevant.

4.3. Shortcomings and Prospects

Undeniably, policy factors have an important impact on the development of artificial oases. From 2006 to 2020, various ecological protection measures such as returning farmlands to forests and desertification control were implemented in Xinjiang [14,31,62], which have greatly influenced the distribution pattern of artificial oases in the territory. On the one hand, fallowing has turned some cultivated artificial oases into unused land or natural oases. On the other hand, after treatment, the area of soil erosion in Xinjiang in 2019 was about 839,800 km^2, which was 45,600 km^2 less than that in 2012 [31], and desertification control has changed some land from desert to natural oases [63,64], which, in turn, have the possibility of being developed into artificial oases. Additionally, priority development areas with favorable policies and the significant deployment of policy needs will lead to urban and population relocation, resulting in a significant increase in the area of artificial oases represented by built-up land. In addition to policy factors, anthropogenic demand factor is another major factor affecting the area of artificial oases [14,65,66], which is reflected in the change in arable land due to the population's demand for food [2,47,67] and accelerated demand for the expansion of construction land due to the development of cities [68,69]. This study only analyzed the potential of development and the utilization of artificial oases in different subsurface environments from the perspective of comprehensive natural geographic background based on morphogenetic geomorphology, which could not offer a completely accurate prediction of future development and could only be used as a reference for site selection in these environments. In future studies, considerations of anthropogenic needs and policy factors can be included to improve the accuracy of the potential estimation.

This study analyzed the development patterns and coupling mechanisms statistically based on the development data of artificial oases in the last 30 years, which could not fully explain the suitability mechanism of each landform. With the development of technology, the land of some landform types may be changed from unsuitable to suitable for develop-

ment, and the conclusions of this study are only appropriate to the current technological level of agro-urban development.

In future research, on the basis of morphogenetic geomorphology, we will combine natural, humanistic, and social data, and, at the same time, improve the accuracy of land-use data by combining indoor and outdoor data with fieldwork to analyze the potential mechanism and development direction of artificial oases in arid zones at a finer scale, with a view towards providing technical support for the development of arid zones.

5. Conclusions

By analyzing the spatio-temporal relationship between morphogenetically coupled landform types and the development of artificial oases in Xinjiang, this study explored the development of artificial oases in different landforms and examined their distribution across the entire territory of Xinjiang over the past 30 years, as well as the suitability of different landforms for the development of artificial oases based on their location. The following conclusions are drawn based on our results:

(1) From 1990 to 2020, the area of artificial oases throughout the territory continued to increase, with a clear trend of expansion to the south due to the development of artificial oases in the southern border from 2005 to 2010, and the center of gravity of these oases continued to migrate in the northeast direction in the other periods.

(2) With regard to the landform–artificial oasis change index, the hierarchical clustering method based on calculating the average Euclidean distance between groups was used to classify the indicators into groups of change trend indicators, change contribution indicators, and exploitation degree indicators according to their similarity, and six types of landform–artificial oasis development suitability models were created based on the results of the clustering analysis, namely, class I suitability (fluvial alluvial plains), class II suitability (fluvial alluvial plains), high-speed suitability (fluvial alluvial terraces), mature suitability (loess terraces and loess plains), low level of suitability, and marginal suitability. Among them, the proportions of landforms of first- and second-class suitability in the whole territory were 7.39% and 6.15%, respectively.

(3) The optimal scale of analysis during the 30-year development of artificial oases in Xinjiang was 8 km, which could explain more than 96% of the growth changes in artificial oases, and the distribution of landforms of class I and class II suitability within the 8km buffer zone of an artificial oasis accounted for 10.55% and 9.90%, respectively, in 2020, and the landforms of class I suitability for the development of artificial oases were mainly concentrated in the north and south of the urban agglomerations on the northern and southern slopes of the Tianshan Mountains, and urban agglomerations located at the southern edge of the Altai Mountain. The suitability of the landforms in the Tuha Basin was mainly of the second level.

Author Contributions: Conceptualization, K.S. and W.C.; methodology, K.S.; software, K.S. and B.W.; validation, K.S., H.X. and Y.Z.; formal analysis, K.S.; data curation, K.S. and R.W.; writing—original draft preparation, K.S. and W.C.; writing—review and editing, K.S., H.X., B.W. and Y.Z.; visualization, K.S.; supervision, W.C.; project administration, W.C.; funding acquisition, W.C. All authors have read and agreed to the published version of the manuscript.

Data Availability Statement: Multi-period land-use/land-cover remote sensing data were obtained from the Resource and Environment Science Data Center of the Chinese Academy of Sciences and the Global Surface Cover Data Product Service website of the National Center for Basic Geographic Information (http://www.resdc.cn, accessed on 17 February 2022).

Conflicts of Interest: The authors declare no conflicts of interest.

References

1. Wang, T.; Wang, Z.; Guo, L.; Zhang, J.; Li, W.; He, H.; Zong, R.; Wang, D.; Jia, Z.; Wen, Y. Experiences and challenges of agricultural development in an artificial oasis: A review. *Agric. Syst.* **2021**, *193*, 103220. [CrossRef]
2. Zhang, J.; Zhang, P.; Gu, X.; Deng, M.; Lai, X.; Long, A.; Deng, X. Analysis of Spatio-Temporal Pattern Changes and Driving Forces of Xinjiang Plain Oases Based on Geodetector. *Land* **2023**, *12*, 1508. [CrossRef]
3. Sun, F.; Wang, Y.; Chen, Y.; Li, Y.; Zhang, Q.; Qin, J.; Kayumba, P.M. Historic and Simulated Desert-Oasis Ecotone Changes in the Arid Tarim River Basin, China. *Remote Sens.* **2021**, *13*, 647. [CrossRef]
4. Gao, P.; Kasimu, A.; Zhao, Y.; Lin, B.; Chai, J.; Ruzi, T.; Zhao, H. Evaluation of the Temporal and Spatial Changes of Ecological Quality in the Hami Oasis Based on RSEI. *Sustainability* **2020**, *12*, 7716. [CrossRef]
5. Li, Z.; Chen, Y.; Zhang, Q.; Li, Y. Spatial patterns of vegetation carbon sinks and sources under water constraint in Central Asia. *J. Hydrol.* **2020**, *590*, 125355. [CrossRef]
6. Liu, Y.; Li, L.; Chen, X.; Zhang, R.; Yang, J. Temporal-spatial variations and influencing factors of vegetation cover in Xinjiang from 1982 to 2013 based on GIMMS-NDVI3g. *Glob. Planet. Change* **2018**, *169*, 145–155. [CrossRef]
7. Zhang, Q.; Sun, C.; Chen, Y.; Chen, W.; Xiang, Y.; Li, J.; Liu, Y. Recent Oasis Dynamics and Ecological Security in the Tarim River Basin, Central Asia. *Sustainability* **2022**, *14*, 3372. [CrossRef]
8. Zhang, Z.; Xu, E.; Zhang, H. Complex network and redundancy analysis of spatial–temporal dynamic changes and driving forces behind changes in oases within the Tarim Basin in northwestern China. *Catena* **2021**, *201*, 105216. [CrossRef]
9. Luo, G.; Feng, Y.; Zhang, B.; Cheng, W. Sustainable land-use patterns for arid lands: A case study in the northern slope areas of the Tianshan Mountains. *J. Geogr. Sci.* **2010**, *20*, 510–524. [CrossRef]
10. Feng, Y.; Luo, G.; Lu, L.; Zhou, D.; Han, Q.; Xu, W.; Yin, C.; Zhu, L.; Dai, L.; Li, Y.; et al. Effects of land use change on landscape pattern of the Manas River watershed in Xinjiang, China. *Environ. Earth Sci.* **2011**, *64*, 2067–2077. [CrossRef]
11. Aspinall, R. Modelling land use change with generalized linear models—A multi-model analysis of change between 1860 and 2000 in Gallatin Valley, Montana. *J. Environ. Manag.* **2004**, *72*, 91–103. [CrossRef] [PubMed]
12. Liu, Y.; Zhang, X.; Lei, J.; Zhu, L. Urban expansion of oasis cities between 1990 and 2007 in Xinjiang, China. *Int. J. Sustain. Dev. World Ecol.* **2010**, *17*, 253–262. [CrossRef]
13. Bai, J.; Chen, X.; Li, L.; Luo, G.; Yu, Q. Quantifying the contributions of agricultural oasis expansion, management practices and climate change to net primary production and evapotranspiration in croplands in arid northwest China. *J. Arid Environ.* **2014**, *100–101*, 31–41. [CrossRef]
14. Zhang, Q.; Yan, M.; Zhang, L.; Shao, W.; Chen, Y.; Dong, Y. Three Decades of Oasis Transition and Its Driving Factors in Turpan–Hami Basin in Xinjiang, China: A Complex Network Approach. *Remote Sens.* **2024**, *16*, 465. [CrossRef]
15. Lamqadem, A.; Saber, H.; Pradhan, B. Quantitative Assessment of Desertification in an Arid Oasis Using Remote Sensing Data and Spectral Index Techniques. *Remote Sens.* **2018**, *10*, 1862. [CrossRef]
16. Boali, A.; Bashari, H.; Jafari, R. Evaluating the potential of Bayesian networks for desertification assessment in arid areas of Iran. *Land Degrad. Dev.* **2018**, *30*, 371–390. [CrossRef]
17. Yang, G.; Li, F.; Chen, D.; He, X.; Xue, L.; Long, A. Assessment of changes in oasis scale and water management in the arid Manas River Basin, north western China. *Sci. Total Environ.* **2019**, *691*, 506–515. [CrossRef] [PubMed]
18. Lei, Y.; Li, X.; Ling, H. Model for calculating suitable scales of oases in a continental river basin located in an extremely arid region, China. *Environ. Earth Sci.* **2014**, *73*, 571–580. [CrossRef]
19. Ling, H.; Xu, H.; Fu, J.; Fan, Z.; Xu, X. Suitable oasis scale in a typical continental river basin in an arid region of China: A case study of the Manas River Basin. *Quat. Int.* **2013**, *286*, 116–125. [CrossRef]
20. Zhang, P.; Deng, M.; Long, A.; Deng, X.; Wang, H.; Hai, Y.; Wang, J.; Liu, Y. Coupling analysis of social-economic water consumption and its effects on the arid environments in Xinjiang of China based on the water and ecological footprints. *J. Arid Land* **2020**, *12*, 73–89. [CrossRef]
21. Sun, D.; Yu, X.; Liu, X.; Li, B. A new artificial oasis landscape dynamics in semi-arid Hongsipu region with decadal agricultural irrigation development in Ning Xia, China. *Earth Sci. Inform.* **2015**, *9*, 21–33. [CrossRef]
22. Li, J.; Feng, Q.; Guo, Q. Fractal study of sustainable proportions of natural and artificial oases. *Environ. Geol.* **2008**, *55*, 1396. [CrossRef]
23. Zhang, Q.; Xu, H.; Li, Y.; Fan, Z.; Zhang, P.; Yu, P.; Ling, H. Oasis evolution and water resource utilization of a typical area in the inland river basin of an arid area: A case study of the Manas River valley. *Environ. Earth Sci.* **2011**, *66*, 683–692. [CrossRef]
24. Yao, K.; Halike, A.; Chen, L.; Wei, Q. Spatiotemporal changes of eco-environmental quality based on remote sensing-based ecological index in the Hotan Oasis, Xinjiang. *J. Arid Land* **2022**, *14*, 262–283. [CrossRef]
25. Song, Q.; Hu, B.; Peng, J.; Bourennane, H.; Biswas, A.; Opitz, T.; Shi, Z. Spatio-temporal variation and dynamic scenario simulation of ecological risk in a typical artificial oasis in northwestern China. *J. Clean. Prod.* **2022**, *369*, 133302. [CrossRef]
26. Liu, Y.; Hu, W.; Wang, S.; Sun, L. Eco-environmental effects of urban expansion in Xinjiang and the corresponding mechanisms. *Eur. J. Remote Sens.* **2020**, *54*, 132–144. [CrossRef]
27. Cai, T.; Zhang, X.; Xia, F.; Zhang, Z.; Yin, J.; Wu, S. The Process-Mode-Driving Force of Cropland Expansion in Arid Regions of China Based on the Land Use Remote Sensing Monitoring Data. *Remote Sens.* **2021**, *13*, 2949. [CrossRef]
28. Waldron, B.; Gui, D.; Liu, Y.; Feng, L.; Dai, H. Assessing water distribution and agricultural expansion in the Cele Oasis, China. *Environ. Monit. Assess.* **2020**, *192*, 288. [CrossRef] [PubMed]

29. Li, B.; Gui, D.; Xue, D.; Liu, Y.; Ahmed, Z.; Lei, J. Analysis of the Expansion Characteristics and Carrying Capacity of Oasis Farmland in Northwestern China in Recent 40 Years. *Agronomy* **2022**, *12*, 2448. [CrossRef]
30. Zhang, Y.; Yang, D.; Zhang, X.; Dong, W.; Zhang, X. Regional structure and spatial morphology characteristics of oasis urban agglomeration in arid area —A case of urban agglomeration in northern slope of Tianshan Mountains, Northwest China. *Chin. Geogr. Sci.* **2009**, *19*, 341–348. [CrossRef]
31. Xia, N.; Hai, W.; Tang, M.; Song, J.; Quan, W.; Zhang, B.; Ma, Y. Spatiotemporal evolution law and driving mechanism of production–living–ecological space from 2000 to 2020 in Xinjiang, China. *Ecol. Indic.* **2023**, *154*, 110807. [CrossRef]
32. Aizizi, Y.; Kasimu, A.; Liang, H.; Zhang, X.; Zhao, Y.; Wei, B. Evaluation of ecological space and ecological quality changes in urban agglomeration on the northern slope of the Tianshan Mountains. *Ecol. Indic.* **2023**, *146*, 109896. [CrossRef]
33. Chidi, C.L. Geomorphic determinanats of landuse intensity. *Int. Arch. Photogramm. Remote Sens. Spat. Inf. Sci.* **2014**, *XL-8*, 703–707. [CrossRef]
34. Hao, L.; Su, X.; Singh, V.P.; Zhang, L.; Zhang, G. Suitable oasis and cultivated land scales in arid regions based on ecological health. *Ecol. Indic.* **2019**, *102*, 33–42. [CrossRef]
35. Cheng, W. *Geomorphological Patterns and Effects in Xinjiang*; Science Press: Beijing, China, 2018.
36. Cheng, W.; Zhou, C.; Li, B.; Shen, Y. Geomorphological regionalization theory system and division methodology of China. *Acta Geogr. Sin.* **2019**, *74*, 839–856.
37. Chang, X.; Xing, Y.; Wang, J.; Yang, H.; Gong, W. Effects of land use and cover change (LUCC) on terrestrial carbon stocks in China between 2000 and 2018. *Resour. Conserv. Recycl.* **2022**, *182*, 106333. [CrossRef]
38. Ning, J.; Liu, J.; Kuang, W.; Xu, X.; Zhang, S.; Yan, C.; Li, R.; Wu, S.; Hu, Y.; Du, G.; et al. Spatiotemporal patterns and characteristics of land-use change in China during 2010–2015. *J. Geogr. Sci.* **2018**, *28*, 547–562. [CrossRef]
39. Zhou, C.; Cheng, W.; Qian, J. *Digital Geomorphological Interpretation and Mapping from Remote Sensing*; Science Press: Beijing, China, 2009.
40. Zhang, L.; Fang, C.; Zhao, R.; Zhu, C.; Guan, J. Spatial-temporal evolution and driving force analysis of eco-quality in urban agglomerations in China. *Sci. Total Environ.* **2023**, *866*, 161465. [CrossRef]
41. Mann, H.B. Nonparametric Tests Against Trend. *Econometrica* **1945**, *13*, 245–259. [CrossRef]
42. Xifeng, J.; Junling, H.; Qi, Z.; Saitiniyazi, A. Evolution pattern and driving mechanism of eco-environmental quality in arid oasis belt—A case study of oasis core area in Kashgar Delta. *Ecol. Indic.* **2023**, *154*, 110866. [CrossRef]
43. Burgos, V.; Jenkins, S.F.; Bono Troncoso, L.; Perales Moya, C.V.; Bebbington, M.; Newhall, C.; Amigo, A.; Prada Alonso, J.; Taisne, B. Identifying analogues for data-limited volcanoes using hierarchical clustering and expert knowledge: A case study of Melimoyu (Chile). *Front. Earth Sci.* **2023**, *11*, 1144386. [CrossRef]
44. Rousseeuw, P.J. Silhouettes: A graphical aid to the interpretation and validation of cluster analysis. *J. Comput. Appl. Math.* **1987**, *20*, 53–65. [CrossRef]
45. Fan, B.; Luo, G.; Hellwich, O.; Shi, X.; Ochege, F.U. Surface deformation detection and attribution in the Mountain-Oasis-Desert Landscape in north Tianshan Mountains. *GIScience Remote Sens.* **2023**, *60*, 2270814. [CrossRef]
46. El-Tantawi, A.M.; Bao, A.; Chang, C.; Liu, Y. Monitoring and predicting land use/cover changes in the Aksu-Tarim River Basin, Xinjiang-China (1990–2030). *Environ. Monit. Assess.* **2019**, *191*, 480. [CrossRef]
47. Zhang, F.; Wang, Y.; Jim, C.Y.; Chan, N.W.; Tan, M.L.; Kung, H.-T.; Shi, J.; Li, X.; He, X. Analysis of Urban Expansion and Human–Land Coordination of Oasis Town Groups in the Core Area of Silk Road Economic Belt, China. *Land* **2023**, *12*, 224. [CrossRef]
48. Shi, G.; Ye, P.; Ding, L.; Quinones, A.; Li, Y.; Jiang, N. Spatio-Temporal Patterns of Land Use and Cover Change from 1990 to 2010: A Case Study of Jiangsu Province, China. *Int. J. Environ. Res. Public Health* **2019**, *16*, 907. [CrossRef]
49. Liu, Z.; Wang, J.; Ding, J.; Xie, X. Analysis of spatial–temporal evolution trends and influential factors of desert-oasis thermal environment in typical arid zone: The case of Turpan–Hami region. *Ecol. Indic.* **2023**, *154*, 110747. [CrossRef]
50. Zheng, F.; Hu, Y. Assessing temporal-spatial land use simulation effects with CLUE-S and Markov-CA models in Beijing. *Environ. Sci. Pollut. Res.* **2018**, *25*, 32231–32245. [CrossRef]
51. Yang, L.; Guan, Q.; Lin, J.; Tian, J.; Tan, Z.; Li, H. Evolution of NDVI secular trends and responses to climate change: A perspective from nonlinearity and nonstationarity characteristics. *Remote Sens. Environ.* **2021**, *254*, 112247. [CrossRef]
52. Xue, J.; Gui, D.; Lei, J.; Sun, H.; Zeng, F.; Mao, D.; Jin, Q.; Liu, Y. Oasification: An unable evasive process in fighting against desertification for the sustainable development of arid and semiarid regions of China. *Catena* **2019**, *179*, 197–209. [CrossRef]
53. Xu, H.; Cheng, W.; Wang, B.; Song, K.; Zhang, Y.; Wang, R.; Bao, A. Effects of Geomorphic Spatial Differentiation on Vegetation Distribution Based on Remote Sensing and Geomorphic Regionalization. *Remote Sens.* **2024**, *16*, 1062. [CrossRef]
54. Zhu, B. The recent evolution of dune landforms and its environmental indications in the mid-latitude desert area (Hexi Corridor). *J. Geogr. Sci.* **2022**, *32*, 617–644. [CrossRef]
55. Wang, L.; Chang, J.; He, B.; Guo, A.; Wang, Y. Analysis of oasis land ecological security and influencing factors in arid areas. *Land Degrad. Dev.* **2023**, *34*, 3550–3567. [CrossRef]
56. Yi, F.; Lu, Q.; Li, Y.; Wang, Z.; Yao, B.; Yang, Q.; Wang, J. Ecological vulnerability assessment of natural oasis in arid Areas: Application to Dunhuang, China. *Ecol. Indic.* **2023**, *149*, 110139. [CrossRef]
57. Saxena, A.; Jat, M.K. Land suitability and urban growth modeling: Development of SLEUTH-Suitability. *Comput. Environ. Urban Syst.* **2020**, *81*, 101475. [CrossRef]

58. Bantayan, N.C.; Bishop, I.D. Linking objective and subjective modelling for landuse decision-making. *Landsc. Urban Plan.* **1998**, *43*, 35–48. [CrossRef]

59. Wang, J.; Zhang, F.; Jim, C.-Y.; Chan, N.W.; Johnson, V.C.; Liu, C.; Duan, P.; Bahtebay, J. Spatio-temporal variations and drivers of ecological carrying capacity in a typical mountain-oasis-desert area, Xinjiang, China. *Ecol. Eng.* **2022**, *180*, 106672. [CrossRef]

60. Lara, M.J.; McGuire, A.D.; Euskirchen, E.S.; Genet, H.; Yi, S.; Rutter, R.; Iversen, C.; Sloan, V.; Wullschleger, S.D. Local-scale Arctic tundra heterogeneity affects regional-scale carbon dynamics. *Nat. Commun.* **2020**, *11*, 4925. [CrossRef]

61. Jahanishakib, F.; Mirkarimi, S.H.; Salmanmahiny, A.; Poodat, F. Land use change modeling through scenario-based cellular automata Markov: Improving spatial forecasting. *Environ. Monit. Assess.* **2018**, *190*, 332. [CrossRef]

62. Lyu, Y.; Shi, P.; Han, G.; Liu, L.; Guo, L.; Hu, X.; Zhang, G. Desertification Control Practices in China. *Sustainability* **2020**, *12*, 3258. [CrossRef]

63. Wu, C.; Lin, Z.; Shao, Y.; Liu, X.; Li, Y. Drivers of recent decline in dust activity over East Asia. *Nat. Commun.* **2022**, *13*, 7105. [CrossRef]

64. Chen, P.; Wang, S.; Liu, Y.; Wang, Y.; Song, J.; Tang, Q.; Yao, Y.; Wang, Y.; Wu, X.; Wei, F.; et al. Spatio-Temporal Dynamics of Aboveground Biomass in China's Oasis Grasslands between 1989 and 2021. *Earth's Future* **2024**, *12*, e2023EF003944. [CrossRef]

65. Guan, Q.; Guan, W.; Yang, J.; Zhao, S.; Pan, B.; Wang, L.; Song, N.; Lu, M.; Li, F. Spatial and temporal changes in desertification in the southern region of the Tengger Desert from 1973 to 2009. *Theor. Appl. Climatol.* **2016**, *129*, 487–502. [CrossRef]

66. Zalles, V.; Hansen, M.C.; Potapov, P.V.; Parker, D.; Stehman, S.V.; Pickens, A.H.; Parente, L.L.; Ferreira, L.G.; Song, X.P.; Hernandez-Serna, A.; et al. Rapid expansion of human impact on natural land in South America since 1985. *Sci. Adv.* **2021**, *7*, eabg1620. [CrossRef]

67. Zhou, D.; Wang, X.; Shi, M. Human Driving Forces of Oasis Expansion in Northwestern China During the Last Decade—A Case Study of the Heihe River Basin. *Land Degrad. Dev.* **2016**, *28*, 412–420. [CrossRef]

68. Arowolo, A.O.; Deng, X. Land use/land cover change and statistical modelling of cultivated land change drivers in Nigeria. *Reg. Environ. Change* **2017**, *18*, 247–259. [CrossRef]

69. Guo, S.; Wang, Y.; Shen, G.Q.P.; Zhang, B.; Wang, H. Virtual built-up land transfers embodied in China's interregional trade. *Land Use Policy* **2020**, *94*, 104536. [CrossRef]